

# Defect Detection in Friction Stir Welding by Online Infrared Thermography

Igor Kryukov\*<sup>†</sup>, Michael Hartmann\*, Stefan Böhm\*, Malte Mund\*\*, Klaus Dilger\*\*  
and Fabian Fischer\*\*

\*Department for Cutting and Joining (tff), University of Kassel, 34125 Kassel, Germany

\*\*Institute of Joining and Welding (ifs), University of Braunschweig, 38106 Braunschweig, Germany

<sup>†</sup>Corresponding author : i.kryukov@uni-kassel.de

(Received July 12, 2014 ; Accepted July 23, 2014)

## Abstract

Friction Stir Welding (FSW) is a complex process with several mutually interdependent parameters. A slight difference from known settings may lead to imperfections in the stirred zone. These inhomogeneities affect on the mechanical properties of the FSWed joints. In order to prevent the failure of the welded joint it is necessary to detect the most critical defects non-destructive. Especially critical defects are wormhole and lack of penetration (LOP), because of the difficulty of detection.

Online thermography is used process-accompanying for defect detecting. A thermographic camera with a fixed position relating to the welding tool measures the heating-up and the cool down of the welding process. Lap joints with sound weld seam surfaces are manufactured and monitored. Different methods of evaluation of heat distribution and intensity profiles are introduced.

It can be demonstrated, that it is possible to detect wormhole and lack of penetration as well as surface defects by analyzing the welding and the cooling process of friction stir welding by passive online thermography measurement. Effects of these defects on mechanical properties are shown by tensile testing.

**Key Words :** Friction Stir Welding (FSW), Non-destructive testing (NDT), infrared thermography, online process monitoring, defect detection, quality of joint

## 1. Introduction

The friction stir welding (FSW) is an innovative pressure welding process which was developed in 1991 at the TWI (The Welding Institute, England). A rotating tool is moved through the workpieces and heats these by friction to shortly below the melting point. Afterwards, the materials, that are to be joined, are stirred, resulting in a metallic connection. An important advantage of the FSW is that no auxiliaries or additive materials are necessary for this process. Furthermore, the preferential use of low melting metals like aluminium and magnesium creates a strong interest in the FSW for applications in

the light weight construction.

The FSW is a process with a lot of interacting parameters which are divided in tool and process parameters. Variations of known setting can lead to diverse irregularities in the weld seam<sup>1)</sup>. These anomalies reduce the bending and breaking strength of the friction stir welded joint. To avoid the failure of weld joints and to secure a consistent weld quality, it is necessary to detect critical defects non-destructive. An adequate non-destructive testing should offer a quick availability of test results as well as the possibility to perform a 100% inspection of the welds.

For the FSW, the infrared thermography serves as an instrument for the online non-

destructive testing. By this means, the infrared radiation of the examined object is measured contact free. Irregularities in the weld seam can already be distinguished due to minor differences in the temperature on the object surface. Defects in the test object lead to a reduced temperature flow, which is the reason why the surface temperature is locally higher than in adjoining regions. The advantages of thermography are the high exactness when measuring large areas online. Due to the short measurement time, the reactionless process offers high automation potential<sup>2,3)</sup>.

Thermography has already been used multiple times with the friction stir welding. Mainly, it was used for the examination of the temperature distribution during the process<sup>4-7)</sup>. Lahiri et al. examined a primed friction stir welded joint by using the optically excited lock-in thermography. By identifying the inserted wormholes they concluded that the infrared thermography can generally be used as a non-destructive testing technology for weld joints<sup>8)</sup>. Dehelean et al. succeeded in proving the existence of simulated surface defects during the friction stir welding by using a thermography camera<sup>9)</sup>. So far, nobody managed to detect the existence of internal defects online and to define the defects.

In this article, thermography is used to detect internal defects in the lap joint of friction stir welded joints. In order to achieve this, sound and defected welds are compared with each other. On the basis of the cooling behaviour of the weld as well as of the temperature development in the process, conclusions can be drawn with regard to defects during the welding process.

## 2. Experimental details

### 2.1 Experimental setup

Lap joints of the aluminium alloy EN AW 6082-T6 (AlMgSi1) are examined on aluminium plates with the measures 500mm × 120mm × 2mm (see table 1 for the chemical composition). The weld seam length is 250mm.

**Table 1** Chemical composition of used aluminium alloy

	Si	Fe	Cu	Mn	Mg	Cr	Zn	Ti
6082-T6	1.00	0.38	0.10	0.52	0.70	0.04	0.05	0.03

An infrared camera is chosen for the thermography measurement during the process and firmly positioned relating to the welding tool. The FLIR SC5600-M is used as the thermography camera. This actively cooled camera with an indium antimonide sensor is distinguished for FSW due to a high resolution of 640 pixels × 512 pixels, a radiography rate of 100Hz, as well as a spectral range of 2.5 $\mu$ m – 5.1 $\mu$ m. Due to the noise equivalent temperature difference (NETD) of less than 20mK, this camera is especially suited for the detection of the smallest temperature differences<sup>10)</sup>. With the help of a construction, the camera is positioned directly over the weld seam to ensure that the distance to the weld seam always stays the same. Due to the tracking of the tool, the cooling process of a constantly large area (min. 90mm × 100mm) can be monitored and evaluated. The distance between the objective and the tool  $r$  is about 270mm, the inclination angle of the camera  $\phi$  relating to the weld level is about 55°, as shown in Fig. 1. The entire welding process has been recorded and evaluated.

To avoid disturbing reflections of the surroundings or the welding machine, the welding area as well as the elements located there are encapsulated, or the surfaces are dyed dull black. However, the aluminium plates deliberately stay undyed. Due to the strong self-heating, the tool emits a lot of heat to the outside. As the aluminium plates are undyed and as they have a very high reflection coefficient, a measurement

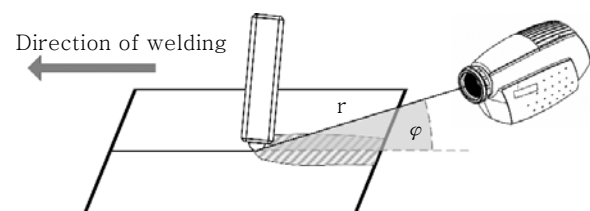


**Fig. 1** Position of thermographic camera relating to the welding tool

of the area directly surrounding the tool is strongly distorted. In order to keep this area out of the measurement, the tool including the tool holding device was encased with a thin walled, dull black hollow cylinder which almost reaches the aluminium plates. It can absorb most of the radiation. Thus, the heat radiating from the tool is mostly isolated from the measurement. Only a small part of residual radiation can be seen on the edge of the hollow cylinder.

## 2.2 Imperfections in FSW

Significant irregularities in the friction stir welding are defined by the AWS D17.3/D17.3M: 2010<sup>11)</sup> as well as DIN EN ISO 25239-5<sup>12)</sup>. Among the most crucial defects are internal defects, like wormholes and the lack of penetration (LOP), which cannot be detected by a simple visual inspection. These defects influence the static and dynamic strength of the weld seam. Other than the thermography, no testing method can detect these defects online.

A wormhole (also referred as cavities or voids) results from insufficient material flow during the process. Due to low rotational speeds and high feed rates, not enough heat is inserted in the weld seam. In case of such a cold weld, a tunnel is generated on the advancing side which is continuing along the weld.

A "lack of penetration" (LOP) is the consequence of an inadequate mixture of the workpieces at the root of the weld. The reason for this is the insufficient plunge depth of the pin into the material. While this defect can be detected in case of a butt joint by inspecting of the reverse side, it is not possible to identify this type of defect in case of a lap joint.

By varying the weld parameters, both sound welds and welds with wormholes as well as "lack of penetrations" have been generated. Two different parameters have been chosen for the "lack of penetration", variant 1 with barely a penetration and variant 2 where the workpieces are not connected to each other. The used weld parameters are shown in table 2. The used tools have a concave shoulder with a diameter of 10mm and a cylindrical pin with a diameter of 4mm. The tools are adjusted to a counter-clockwise rotation (negative rotation speed, see table 2) and have a thread support to improve the material flow.

With regard to the wormholes, the rotating direction has been changed from counter-clockwise to clockwise (positive rotation speed, see table 2). Furthermore, the rotation speed has been reduced and the feed rate increased. To generate the "lack of penetration", a tool with a shortened pin has been used. Additionally, the plunge depth has been reduced. With these parameters, it has been ensured that the welds seem to be sound on the outside despite the inserted defects. Fig. 2 shows the produced welds a) sound weld, b) weld with wormhole, c) "lack of penetration" variation 1, connection still existing, d) "lack of penetration" variation 2, without connection between the workpieces.

## 3. Results and discussion

### 3.1 Evaluation of online measurement

Sound welds as well as weld specimens with the mentioned defects have been successfully produced. Related to the process, thermographic measurements have been made throughout the

**Table 2** Welding parameters

	feed rate [mm/min]	rotation speed [ $\text{min}^{-1}$ ]	tilt angle [ $^{\circ}$ ]	plunge depth [mm]	pin length [mm]
sound weld	800	-1000	2	2.68	2.3
wormhole defect	1000	+800	2	2.68	2.3
lack of penetration v1	800	-1000	2	2.30	2.0
lack of penetration v2	800	-1000	2	2.23	2.0

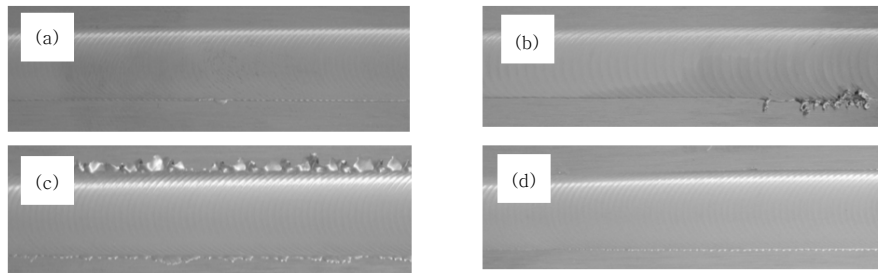


**Fig. 2** Surface of welded joints: (a) sound weld, (b) weld containing wormhole defect, (c) lack of penetration defect v1 (with connection between workpieces), (d) lack of penetration defect v2 (without connection between workpieces)

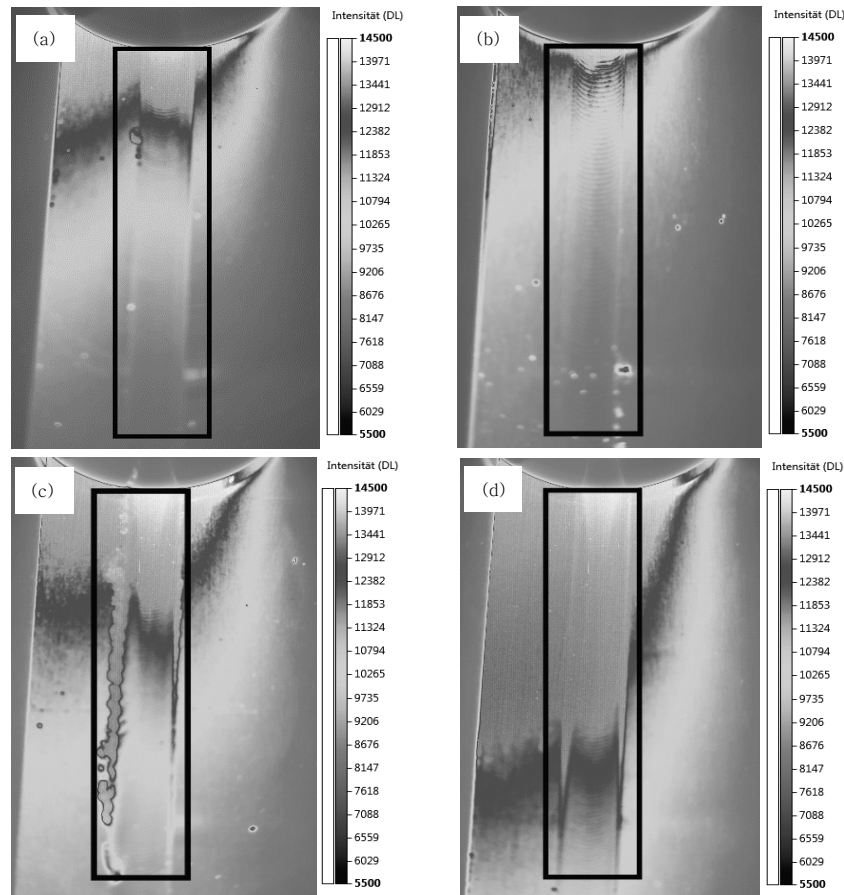


**Fig. 3** Thermographic exposure in the welding process: (a) sound weld, (b) weld containing wormhole defect, (c) lack of penetration defect v1 (with connection between workpieces), (d) lack of penetration defect v2 (without connection between workpieces)

whole process. Infrared images of the single weld tests are presented in Fig. 3. In the centre, the imbricated weld can be seen which proceeds from the bottom to the top. Above it, the mentioned hollow cylinder can be seen which does not radiate or reflect heat. On the left of the weld, the edge of the plate is distinctly visible. The defective heat conduction leads to a heating

of the plate edge, while the aluminium plate lying below is considerably less influenced by the heat. The single, round heat sources, as well as the heat sources along the weld are flashes, which were generated during the process. Flashing and other surface defects are a major problem for the thermography. As these defects have a higher heat radiation than the weld seam, the

lower lying defects are overlaid at this position and, consequently, not discernible.

To achieve a better comparability of the single thermography images, they have been equally scaled. It is impossible to display the absolute temperature of the weld seam at this position. The reason for this is the not exactly known but low emissivity of the workpieces. However, this is not important for the evaluation. The scale describes a dimensionless intensity quantity. As each measurement has been made under the same conditions, the measured intensity distributions can be compared directly with each other.

A first comparison of the thermographic images at any time during the process already provides first insights. The thermography image of the sound weld serves as a reference for further comparisons. The temperature distribution of the weld seam with the wormhole (see Fig. 3 b)) shows low intensity compared with the sound weld seam. This suggests a cold weld. The uneven intensity distribution along the weld seam suggests a continuous wormhole. Other cold weld defects change the seam surface and can be easily detected by strong local increase of intensity or even visual inspection. The shortened pin in Fig. 3 c) still leads to a joining of the workpieces. The thermographic image shows a similar result as the reference weld. Only the stated intensities display slightly higher data. In comparison to that, it is possible to detect a heat accumulation on the surface in Fig. 3 d). The heat generated during the process cannot flow off into the lower workpiece which can be attributed to a "lack of penetration".

### 3.2 Evaluation of intensity profiles

For a more distinct evaluation, a quadratic area around the weld seam has been chosen during each measurement, and the measured intensities have been examined. The area has a size of 100 pixels  $\times$  450 pixels and complies with an evaluated weld seam area of about 20mm  $\times$  80mm. This area is encircled by the black mark in Fig. 3.

At first, the cooling behaviour of the weld seams during the process, shown in Fig. 3 a) to 3 d), has been evaluated. Thereby, the average intensities along each row with the same distance to the sheath within the mark have been determined. The cooling behaviour of the welds is demonstrated in Fig. 4. Defects caused by flashes on the surface in form of sudden temperature rises can be easily distinguished due to the intensity profiles.

The almost linear intensity profile of the reference weld can be clearly recognized. A sound weld proportionally cools down with increasing distance to the tool. In case of the cold weld, less heat is inserted into the weld. Though the temperature shortly after the welding process is almost as high as in other welding processes, this weld cools down exponentially. With regard to the lack of penetration variant 1, the completely welded area is considerably smaller compared with the reference weld. The reduced area lowers the heat conduction into the lowest aluminium plate, causing a slower but nevertheless linear decline of temperature and intensity. Compared to that, there is no connection between both workpieces in case of the lack of penetration variant 2. The produced heat can only be spread within the upper aluminium plate. Due to the smaller material volume and the smaller surface, the cooling down is slower, which can be seen in Fig. 4.

In addition to the evaluation of the single thermography images at particular points in time, the intensity distribution over the whole weld process has been evaluated. In order to

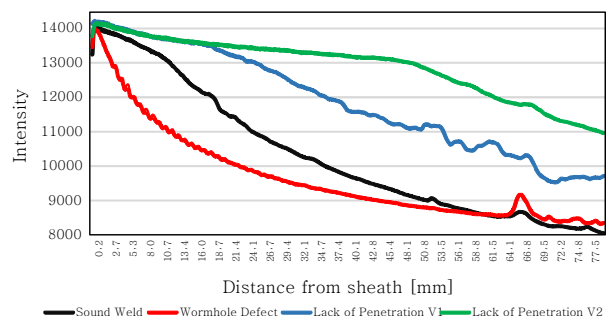
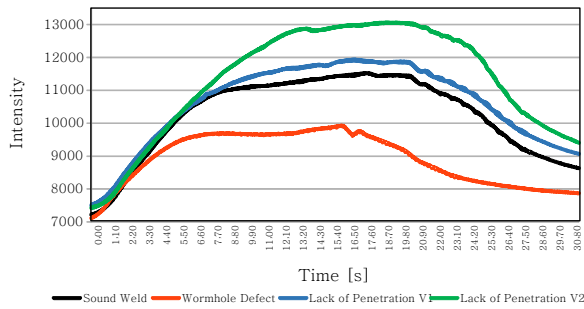


Fig. 4 Intensity profiles on the basis of figure 3: mean intensity value per distance at an optional time



**Fig. 5** Intensity profiles during the welding process: mean intensity value development during the total welding process

achieve this, an average intensity value has been created from the 45,000 measurement data per measurement image. The resulting intensity profiles are shown in Fig. 5. An initially strong temperature increase is visible, where the workpieces have been heated to weld temperature. Afterwards, a lower temperature increase ensued during the welding process. The maximum temperature is reached at the end of the weld. Due to the higher feed rate, the maximum temperature is reached faster if it is a wormhole than in case of the other welds. From this point in time the joined plates cool down.

The intensity profiles over the whole duration of the weld process confirm the already achieved insights. Compared to the sound weld, the average intensity of the weld with wormholes is about 15% lower. While the lack of penetration variant 1, just shows a 5% higher intensity, it is 10% to 15% higher for lack of penetration variant 2, than the reference value.

In order to examine the results with regard to the reproducibility, each weld test has been repeated three times with the correspondent parameters. Despite of the intensity variation by 2-3%, each result, the thermography images as well as the intensity profiles have been reproducible. Consequently, it is possible, to infer from the thermography images and the intensity profiles of the weld that there are wormholes or a lack of penetration.

### 3.3 Destructive evaluation

In order to validate the results, destructive

test has been made with the specimens. Two specimens have been removed from each weld specimen to execute the tensile test and the microscopic analysis, as it is shown in Fig. 6. It was not possible to take specimens of the lack of penetration variant 2, as these directly disintegrated during the removal due to the non-existing penetration.

Microscopic analyses have been made of the specimens to validate the results. Under the microscope, there are no defects visible in the sound weld (see Fig. 7). However, it is relatively easy to distinguish the centered wormhole (length about  $2848\mu\text{m}$ , width about  $264\mu\text{m}$ ), also detectable in Fig. 3 b).

At the end, simplified tensile tests were executed

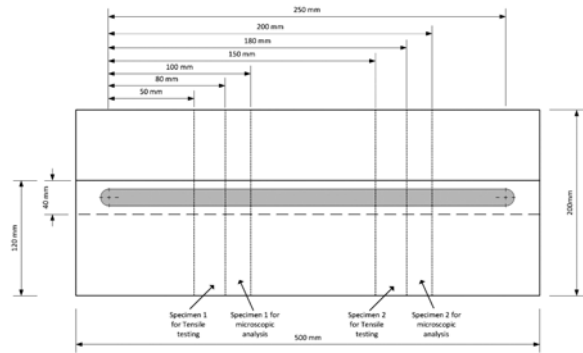


**Fig. 6** Location of removal of the specimen (drawing without scale)

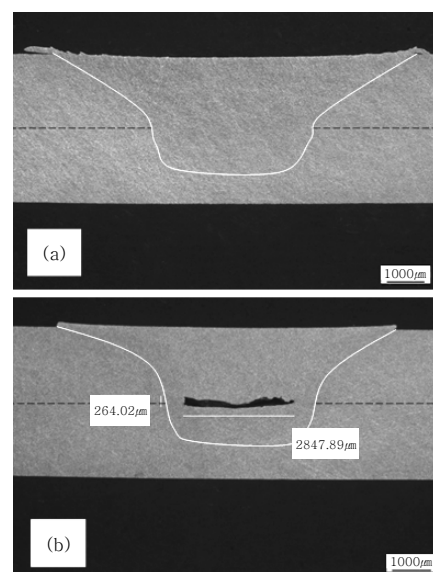


**Fig. 7** Metallographic confirmation for accurate seam (a) and wormhole defect (b)

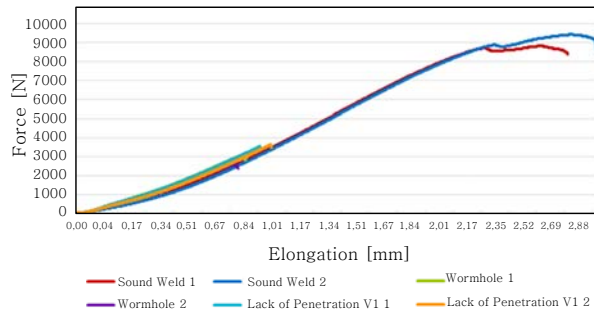


**Fig. 8** Tensile testing of defective and sound weld seams

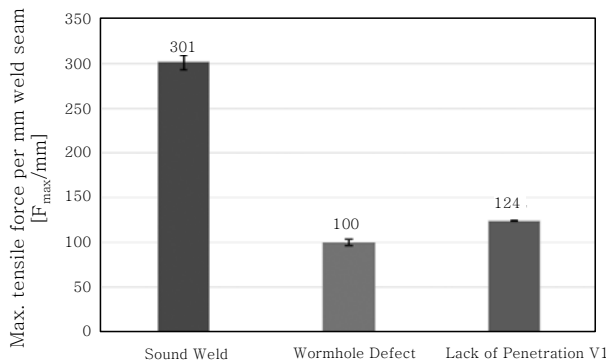


**Fig. 9** Maximal tensile force per mm weld seam for defective and accurate specimen

on the diverse specimens. They shall demonstrate the influence of detected defects on the tensile strength. With regard to the simplification, the maximum tensile forces have been examined. The progress of the tensile tests is demonstrated in Fig. 8.

The tensile tests demonstrate that the inserted defects considerably reduce the maximum tensile forces. The maximum force per mm weld seam of the specimen of the regular weld seam is about 301N/mm, the specimen of the wormhole is at about 100N/mm (about 33% of the regular seam) and the one of the lack of penetration variant 1 lies at about 124N/mm (about 41% of the regular seam), as it is shown in Fig. 9. Contrary to the defected specimens, both accurate tension tests failed outside the weld seam.

#### 4. Conclusions

In this article, the first results of the current project, aiming at the confirmation of the suitability of the thermography as a non-destructive

testing method, have been demonstrated. During the course of the project it shall be proven that internal defects, like wormholes and “lack of penetration”, occurring in the friction stir welding can be detected during the cooling process. This shall enable a process-related control of the weld seam.

The most important results of this article are:

- Thermography can be used with the friction stir welding to examine the heating and cooling progress of weld seams
- A good thermal shield from surrounding and process disturbing factors as well as from the tool is compulsory for thermography to reduce disturbances
- Surface defects like flashing distort the thermography measurement due to a higher heat radiation and, consequently, impede the detection of subjacent defects
- By considering the variations of intensity distribution compared to the reference measurement, internal defects like “wormholes” and “lack of penetration” can be detected with online-thermography

During the course of the project it will be examined which further defects can be detected from the intensity profiles. In addition to that the transferability of the results to other geometries and aluminium alloys is tested.

#### Acknowledgement

The authors would like to acknowledge the DVS - Deutscher Verband für Schweißen und verwandte Verfahren e.V. for its financial support via project ThermoFSW (DVS-Nr.: 05.049) and the technical support of all project participants.

#### References

1. W.J. Arbegast: A flow-partitioned deformation zone model for defect formation during friction stir welding, *Scripta Materialia*, **58** (2008), 372-376
2. S. Bagavathiappan, B.B. Lahiri, T. Saravanan, J. Philip, T. Jayakumar: Infrared thermography for condition monitoring - A review, *Infrared Physics & Technology*, **60** (2013), 35-55
3. X.P. Maldague, P.O. Moore: Infrared and Thermal



- Testing - Volume 3: Nondestructive Testing Handbook - Third edition, American Society for Non-destructive Testing, Columbus, 2001
4. A. Forcellese, M. Martarelli, G. Pandarese, M. Simoncini: Similar and Dissimilar FSWed Joints in Lightweight Alloys: Heating Distribution Assessment and IR Thermography Monitoring for On-Line Quality Control, *Key Engineering Materials*, **554-557** (2013), 1055-1064
  5. S. Beccari, L. D'Acquisto, L. Fratini, C. Salamone: Thermal Characterization of Friction Stir Welded Butt Joints, *Advanced Materials Research*, **6-8** (2005), 583-590
  6. C.C. Rusu, L.R. Mistodie: Thermography used in friction stir welding processes, *Welding equipment and technology*, **21** (2010), 62-65
  7. B.M. Darras, M.A. Omar, M.K. Khraisheh: Experimental Thermal Analysis of Friction Stir Processing, *Materials Science Forum*, **539-543** (2007), 3801-3806
  8. B.B. Lahiri, S. Bagavathiappan, T. Saravanan, K.V. Rajkumar, A. Kumar, J. Philip, T. Jayakumar: Defect Detection in Weld Joints by Infrared Thermography, *NDESAI 2011*, 191-197
  9. D. Dehelean, V. Safta, R. Cojocaru, T. Hälker, C. Ciuca: Monitoring the quality of friction stir welded joints by infrared thermography, *Safety and Reliability of Welded Components In Energy and Processing Industry* (2008), 621-626
  10. FLIR Systems, Inc.: FLIR® Silver SC5000 MWIR, Rev. 10/09-R1, URL: <http://www.flir.com/WorkArea/DownloadAsset.aspx?id=20006>
  11. An American National Standard, AWS D17.3/D17.3M:2010, American Welding Society Specification for friction stir welding of aluminum alloys for aerospace applications (2010)
  12. DIN Deutsches Institut für Normung e.V., DIN EN ISO 25239-5: Rührreißschweißen - Aluminium - Teil 5: Qualitäts- und Prüfungsanforderungen (2012)



**Igor Kryukov** received the first graduate engineer and the second graduate engineer in mechatronics from University of Kassel, Germany, in 2010 and 2013. He is a Research Engineer at the Department for Cutting and Joining (tff) at the University of Kassel, Germany.

His current research interests include large-area non-destructive testing (NDT) in the field of welding and bonding.



**Michael Hartmann** received the first graduate engineer and the second graduate engineer in mechatronics from University of Kassel, Germany, in 2011 and 2013.

He is a Research Engineer at the Department for Cutting and Joining (tff) at the University of Kassel, Germany. His current research interests include Friction Stir Welding, tool development and combined process in Friction Stir Welding.



**Stefan Böhm** received the graduate engineer in electrical engineering from TU Darmstadt, Germany, in 1994, and the Ph.D. degree in Mechanical Engineering from RWTH Aachen, in 1999.

From 2002-2010 he was the chair of the Department for Micro joining at the Technical University of Braunschweig. Since 2010, he is the chair of the Department for Cutting and Joining (tff) at the University of Kassel, Germany. The research priorities of the Department for Cutting and Joining are the welding, bonding and cutting technologies.



**Malte Mund** received the diploma degree in mechanical engineering from the University of Paderborn, Germany, in 2011. Since then he works as a research associate at the Institute of Joining and Welding at the TU Braunschweig, Germany. His research interests are non-destructive testing of joints by

thermography, the behavior of joined sandwich structures and debonding of structural adhesive joints.



**Klaus Dilger** received the diploma degree in 1987 and the Ph.D. degree in mechanical engineering in 1991 from the TU München, Germany. In 1997, he became professor of adhesive bonding at the RWTH Aachen, Germany. In 2002 he became head of the Institute of

Joining and welding of the TU Braunschweig, Germany. His research focuses on joining technologies for lightweight materials including material properties, joining processes and quality assurance by means of non destructive testing.



**Fabian Fischer** received his diploma degree in chemistry (2000) as well the Ph.D. degree in chemistry (2007) from the Friedrich Wilhelm Leibniz Universität Hannover, Germany. Since 2011, he is head of the departments of composite materials and beam technologies of the

Institute for Joining and Welding at the TU Braunschweig, Germany which includes the research unit for non destructive testing. His work focuses on laser and electron beam welding, the laser machining of composite materials and the quality assurance of both welded structures and composites.